

# Soft Matter

Accepted Manuscript

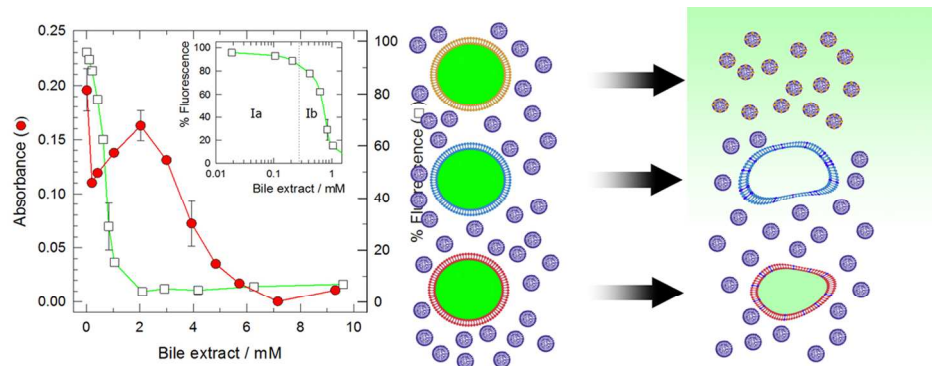


This is an *Accepted Manuscript*, which has been through the Royal Society of Chemistry peer review process and has been accepted for publication.

*Accepted Manuscripts* are published online shortly after acceptance, before technical editing, formatting and proof reading. Using this free service, authors can make their results available to the community, in citable form, before we publish the edited article. We will replace this *Accepted Manuscript* with the edited and formatted *Advance Article* as soon as it is available.

You can find more information about *Accepted Manuscripts* in the [Information for Authors](#).

Please note that technical editing may introduce minor changes to the text and/or graphics, which may alter content. The journal's standard [Terms & Conditions](#) and the [Ethical guidelines](#) still apply. In no event shall the Royal Society of Chemistry be held responsible for any errors or omissions in this *Accepted Manuscript* or any consequences arising from the use of any information it contains.



129x50mm (300 x 300 DPI)

# Characteristics and behaviour of liposomes when incubated with natural bile salt extract: Implications for their use as oral drug delivery systems

5 Laura G. Hermida,<sup>a</sup> Manuel Sabés-Xamaní,<sup>b</sup> Ramon Barnadas-Rodríguez\*<sup>b</sup>

a Centre of Research and Development in Chemistry, National Institute of Industrial Technology (INTI), Av. Gral. Paz e/ Constituyentes y Albarelos San Martín, Buenos Aires, Argentina.

b Centre d'Estudis en Biofísica, Unitat de Biofísica, Departament de Bioquímica i Biologia Molecular. Faculty of Medicine, Universitat Autònoma de Barcelona, 08193 Cerdanyola, Catalonia, Spain.

## Corresponding author

Ramon Barnadas-Rodríguez

15 Centre d'Estudis en Biofísica, Unitat de Biofísica, Departament de Bioquímica i Biologia Molecular. Faculty of Medicine, Universitat Autònoma de Barcelona, 08193 Cerdanyola, Spain.

E-mail: [ramon.barnadas@uab.cat](mailto:ramon.barnadas@uab.cat)

Tel: 0034935868476

20 Fax: 0034935811907

**ABSTRACT**

The use of liposomes for oral administration of drugs and for food applications is based on their ability to preserve entrapped substances and to increase their bioavailability.

25 Bile salts are one of the agents that affect liposome structure during intestinal digestion and the main reported studies on liposome/bile salt systems have been performed using only one bile salt. The aim of this work was to characterise the interaction of liposomes with a natural bile salt extract (BSE) at physiological pH and temperature. Three types of liposomes (fluid, gel-state and liquid-ordered bilayers) were studied. Phase diagrams  
30 were obtained and a very different behaviour was found. Fluid bilayers were completely permeable to an entrapped dye with partial or complete disruption of vesicles (final size 10 nm). Gel-state bilayers released their content but BSE led to the formation of large mixed structures (2,000 nm). Liquid-ordered bilayers formed mixed vesicles (1,000 nm) and, surprisingly, retained a high percentage of their aqueous content (about 50%). As a  
35 consequence, each type of liposome offers singular features to be used in oral applications due to their specific interaction with bile salts.

**Keywords**

Colloids. Oral drug delivery. Bile salts. Intestinal digestion. Phospholipids.

40 Bioavailability.

## 1 INTRODUCTION

Liposomes as (soft) drug delivery systems are commonly used in parenteral and topical  
45 administrations,<sup>1,2</sup> but after a period of uncertainty the oral route potential has now  
emerged.<sup>3-7</sup> Due to their structure, liposomes can protect the entrapped substances from  
the environment of the gastrointestinal tract, and their *in vivo* effectiveness depends on,  
among other factors, the changes that they undergo when they interact with the bile salts  
present in the intestines. In this way, the macromolecular assembly of phospholipids can  
50 undergo several changes that can lead to the total disruption of the vesicles. The role of  
bile salts in the use of liposomes and other colloids as drug carriers is not only limited to  
the digestion process, as it has been shown that the inclusion of some of them in the  
particle structure enhances their pharmacological activity.<sup>8-9</sup>

At the same time, the evaluation of oral formulations to predict their bioavailability and  
55 mucoadhesion properties greatly depends on the existence of *in vitro* models, such as  
the Caco-2 cultures.<sup>10-13</sup> In these cases, and prior to the incubation with cell cultures,  
formulations are usually exposed to *in vitro* digestion that mimics the gastrointestinal  
tract. The intestinal step of the previous process usually requires sample incubation with  
a bile salt extract (BSE) from a biological source.<sup>14-16</sup>

60 Consequently, a detailed knowledge of the processes involved in the interactions of  
liposomes and BSE would contribute to improve the functionality of the oral  
formulations that contain these vesicles. In fact, the effect of bile salts on phospholipid  
bilayers and monolayers is a particular case of the well-known solubilisation process<sup>17-</sup>  
<sup>19</sup> caused by surfactants which involves three different stages: a) during the vesicular  
65 stage the liposome bilayer becomes progressively enriched in the surfactant, b)  
liposomes are gradually destroyed as the surfactant concentration increases and mixed  
micelles are formed and, c) only (mixed) micelles exist in the bulk. Solubilisation

curves can be obtained by monitoring absorbance/turbidity changes in different liposome suspensions upon increasing surfactant concentration. Some characteristic points that indicate the phase boundaries (usually the onset and full solubilisation points) can be observed from these curves. These points are then used to obtain the phase diagram of the system. It is described in the literature that, for a given surfactant, liposome solubilisation depends to a great extent on the size, lamellarity and composition of the vesicles, as well as temperature and ionic strength of the medium.<sup>20-</sup>

<sup>22</sup> Most of the liposome solubilisation studies performed with bile salts have been made using pure molecules such as sodium cholate, sodium deoxycholate, or some artificial mixtures.<sup>23-25</sup> Even though the effect of natural BSE on liposomes implies a closer approximation to the *in vivo* intestinal digestion, and BSE is commonly used in *in vitro* liposome digestion models, to our knowledge there are no detailed studies focused on the effects of natural BSE on these vesicles. Moreover, no detailed studies providing phase diagrams for mixtures of bile salt extracts with liposomes are available. If liposomes are currently intended to be used for oral drug delivery, knowledge of their behaviour in the presence of a complex natural mixture of bile salts could provide important information for the optimisation of the system.

Our work endeavours to fill these gaps in the scientific literature. On the one hand, it analyses and provides a hypothesis, not previously described, about the formation of mixed structures with BSE, especially for the cases of saturated and cholesterol containing liposomes. The phase diagrams of the studied systems are also obtained. We report and analyse the interactions of a natural BSE with three types of liposomes that exhibit very different phase membrane properties at human body temperature (37 °C): a) soy phosphatidylcholine (SPC), which has a negative transition temperature and, therefore, forms fluid bilayers; b) gel-state membranes composed of hydrogenated SPC

(HSPC), with a transition temperature higher than that of the human body, and; c) liquid-ordered bilayers of HSPC and cholesterol 3:2 mol/mol (HSPC/CHOL), which exhibit the characteristics of both fluid and gel phases, and have no transition temperature.<sup>26,27</sup> Consequently, a very different behaviour is expected when they interact with a natural BSE. These lipids are purified by large scale methods, are commercially available, and are usually used by food and pharmaceutical industries. The BSE commercial extract used has a bile salts composition that is very similar to human bile as previously determined.<sup>28-29</sup> The present paper specifically describes the physical evolution of those liposomes at 37°C and pH 6.5 (with no presence of intestinal enzymes) by measuring the turbidity changes of the sample and by dynamic light scattering. From these measurements, phase diagrams were obtained and the temperature was eventually raised to achieve full solubilisation. The capacity of the liposomes to maintain the entrapped aqueous medium was also evaluated by measuring the leakage of pyranine, a non-bilayer permeable fluorescent probe. We found that each type of vesicle exhibits a very different behaviour not only as regards the susceptibility to be fully solubilised by BSE, but also in the vesicular stage. The results set suggests the formation of three different molecular aggregates which, depending on the initially entrapped substances, may determinate the effectiveness of each type of liposome in nutritional formulations.

## 2 EXPERIMENTAL SECTION

### 2.1 Chemicals and reagents

SPC (minimum 95%) and HSPC (minimum 95%) were obtained from Degussa (Germany). BSE (hyocholic acid 5.3%, cholic acid 18.5 %, deoxycholic acid 2.5 %, glyco and taurocholic acid 37.5%, glyco and taurodeoxycholic acid 21.6 %), CHOL ( $\geq$

99%) were purchased from Sigma-Aldrich (USA). Pyranine was from Kodak (USA) and DPX (a pyranine quencher) was from Molecular Probes (The Netherlands). All other reagents were of analytical grade.

## 2.2 Liposome preparation

SPC and HSPC were added into 10 mM TRIS, 145 mM sodium chloride, pH 6.5 buffer solutions (since pH changes during intestinal digestion from, approximately, 5.7 to 7.4, this mean value was selected and used throughout the work) and stirred 60 minutes at 40°C or 55°C respectively. The resulting multilamellar vesicles (33 mM) were further homogenized<sup>30</sup> using a Microfluidizer 110S at the previously indicated temperatures. HSPC/CHOL liposomes were prepared at a lipid molar ratio of 3:2. Lipids were dissolved in chloroform:methanol (2:1 v/v) and solvent was eliminated by rotary-evaporation. The dry film obtained was hydrated with the buffer solution (final lipid concentration 41 mM) and vortexed at 55-60°C before homogenization at the same temperature. When required, 2 mM pyranine (a water soluble fluorescent dye) was added to the buffer.

## 2.3 Vesicle size determination

Particle size was measured by dynamic light scattering (Ultrafine Particle Analyzer UPA150, USA). Cell temperature was controlled by an external bath, and the change of water viscosity with temperature was considered in the software presets. Analyses were performed without sample dilution in order not to alter phase equilibrium. Results are expressed as the mean diameter of the volume distribution and SD ( $n \geq 2$ ).

## 2.4 Solubilisation assays



Solubilisation curves of liposomes at several concentrations were obtained by monitoring sample absorbance (600 nm) on a double beam spectrophotometer Varian CARY 3Bio. The wavelength was chosen in order to minimize the interference of BSE absorption. Appropriate dilutions of the BSE in TRIS buffer (pH 6.5) were used as reference solutions. The required volumes of concentrated BSE aliquots were added to the continuously stirred samples. Results are expressed as mean  $\pm$  SD ( $n \geq 2$ ). The phase diagrams were obtained by calculating the characteristic points of the solubilisation curves. At a given concentration of lipid (each one of the curves), the corresponding BSE concentrations were calculated from the break points of the curve, from its first derivative (0 value) and, in the case of total liposome solubilisation, the BSE concentration that caused an absorbance value equal or smaller than 0.03 was also considered. Results of the phase diagrams are expressed as the mean  $\pm$  SD ( $n \geq 2$ ).

155

### 2.5 Fluorescence assays

Fluorescence assays were performed to study the effect of BSE on the aqueous content of liposomes. Vesicles were obtained in buffer containing pyranine 2 mM and subsequently purified by size exclusion chromatography (Sephadex G-25) to remove the non-entrapped dye. After adjusting the lipid concentration, sample aliquots were incubated during 1 h at 37°C with increasing concentrations of BSE. The percentage of pyranine retention was calculated from the ratio of the corrected fluorescence measured before and after the addition of 150  $\mu$ l of DPX 200 mM to 3 ml of sample. As BSE exhibits intrinsic fluorescence, curves of BSE fluorescence in absence and presence of DPX were acquired for data correction. Fluorescence was measured with a SLM Aminco 8100 Spectrofluorometer using 417 nm and 511 nm as excitation and emission wavelengths respectively. Results are expressed as mean  $\pm$  SD ( $n \geq 2$ ).

165

## 2.6 Differential scanning calorimetry (DSC)

170 The main phase transition temperature of HSPC and HSPC/CHOL liposomes was determined using a Microcal MC-2 DSC microcalorimeter (USA). Measurements were performed at a heating rate of 90°C/h, from 25 to 80°C, and using TRIS buffer as a blank.

## 175 **3 RESULTS**

### 3.1 SPC liposomes

Figure 1 shows the behaviour of SPC vesicles when incubated with BSE for 1 h at 37°C (the absorbance remained constant after 20 minutes of incubation at each BSE concentration, indicating that all the mixtures reached a steady state). The results of  
180 absorbance reflected the morphological changes of liposomes caused by the interaction with BSE. The absorbance curve illustrates the well-known three-stage model for the interaction between liposomes and surfactants:<sup>31</sup> I) bile salt molecules interact with the membranes without disrupting the vesicles (0-2 mM of BSE); II) after saturation of the bilayers, vesicles are progressively solubilised and, concomitantly, mixed micelles are  
185 formed (2 mM to approximately 6 mM of BSE) and; III) only micelles are present in the sample (BSE concentration > 6 mM). It can be observed that stage I (vesicular domain) exhibited particular absorbance changes: There was a clear initial decrease of the absorbance (stage Ia) and a subsequent increase (stage Ib). The fluorescent changes of Fig. 1 indicate that, in one hour, the dye was released at BSE concentrations that did not  
190 cause bilayer disruption, that is, during stage I. This was especially true during stage Ib, as the retention of the dye drastically diminished (inset Fig. 1), and pyranine was almost completely released before the onset of formation of mixed micelles. Figure 2 shows the

absorbance variations of different concentrations of SPC liposomes after the addition of increasing amounts of BSE. From the similarity of the profiles, in all cases, it can be assumed that equivalent morphological changes and processes took place. Several  
 195 characteristic points can be obtained from the curves at different SPC concentrations:  $C_{lab}$ , the BSE concentration that caused the change from stage Ia to stage Ib (minimum absorbance value of stage I);  $C_{sat}$ , the BSE concentration that caused the saturation of the bilayer (limit between stages I and II); And  $C_{sol}$ , the BSE concentration that caused  
 200 full solubilisation of liposomes (limit between stages II and III). The inset of Fig. 2 was obtained by plotting total BSE concentration vs. total lipid concentration at the previously obtained characteristic points. The results parallel the general behaviour of liposome/surfactant systems<sup>17-19, 23</sup> in which, from each family of characteristic points, a linear ansatz can be made using the following general equation:

$$205 \quad [detergent]_T = [detergent]_w + R_e \cdot [Lip]_T \quad \text{Eq. (1)}$$

Where, when applied to the case of BSE,  $[BSE]_T$  is the total BSE concentration,  $[BSE]_w$  is the BSE concentration in the bulk,  $[Lip]_T$  is total lipid concentration, and  $R_e$  is the effective BSE to lipid ratio, that is, the ratio of the total detergent concentration that is bound to the lipids in the different types of mixed aggregates ( $[BSE]_{agg}/[Lip]_{agg}$ ). Each  
 210 one of the previous parameters are used to establish the different phase boundaries of the system. From the previous equation, it is also possible to calculate the molar fraction of BSE in the mixed aggregates,  $x_{agg}^{BSE}$ , that is: <sup>23,32,33</sup>

$$x_{agg}^{BSE} = \frac{[BSE]_{agg}}{[BSE]_{agg} + [Lip]_{agg}} = \frac{R_e}{R_e + 1} \quad (2)$$

The values of the parameters obtained for the relationships are shown in Table 1 and the  
 215 corresponding curves set the limits of the four different stages mentioned previously (Ia, Ib, II and III). As can be observed (inset Fig. 2), in the studied range the  $C_{lab}$  points do

not give a curve with a significant slope and, consequently, a mean value of  $0.41 \pm 0.23$  mM is obtained for  $[\text{BSE}]_{\text{w}}^{\text{lab}}$ . Due to the deviation from linearity, the absorbance of the lower lipid concentration was rejected for the calculation of the saturation phase boundary. Figure 3 shows the variation of the mean diameter of SPC vesicles as a function of total BSE concentration. The results indicate a gradual decrease of vesicle size (initial diameter  $539 \pm 150$  nm) when BSE is added. By the end of the solubilisation process the diameter was consistent with the size of mixed micelles (about 10 nm). As the diameter is expressed in volume percentage, it can be inferred that all the aggregates detected corresponded to micelles, and no other kind of vesicles was present.

### 3.2 HSPC liposomes

The absorbance variation of HSPC liposomes as a function of BSE concentration after 1 h incubation at  $37^\circ\text{C}$  is shown in Figure 4. Results show a different behaviour than that of SPC liposomes. As can be observed, no stage Ia was detected and a high positive slope of the absorbance was obtained at low BSE concentrations. Subsequently, and in a similar way to SPC vesicles, a BSE concentration which corresponded to the onset of solubilisation was achieved (about 3.5 mM). A further increase in the BSE concentration caused a decrease of the absorbance but, contrary to SPC liposomes, it did not lead to a zero value of the absorbance. Instead, the absorbance decreased to a final constant value (about 0.5) that was higher than the initial value (0.2) obtained in the absence of BSE. In the fluorescence assay (Fig. 4), the release of the dye took place at very low concentrations of BSE and there was an almost a complete leakage (90-95%) at a BSE concentration of 0.8 mM (although no vesicle disruption took place). Similar absorbance changes were observed at different phospholipid concentrations (Figure 5) and full solubilisation of liposomes was not attained even at the highest BSE to

phospholipid ratio used. As regards the size measurements performed at a phospholipid concentration of 1.2 mM (Fig. 3), it can be observed that their evolution was concomitant to the absorbance changes at the same concentration and no micelle size was achieved (initial diameter  $800\pm 240$  nm; final diameter  $1800\pm 260$  nm).

In order to achieve full vesicle solubilisation the temperature of the sample had to be raised above the phase transition temperature of HSPC ( $52.2\pm 0.1^\circ\text{C}$ ,  $n=4$ ).

The absorbance results obtained at  $55^\circ\text{C}$  (Figure 6) for the two higher phospholipid concentrations (3.3 and 2.1 mM) were quite similar to the curves of SPC liposomes at  $37^\circ\text{C}$ . They showed an initial decrease of the absorbance and a subsequent increase before the onset of solubilisation. Then, in those cases and as for SPC, the vesicular domain of the fluid bilayers of HSPC exhibited the stages Ia and Ib in the presence of BSE. But for lower phospholipid concentrations the shape of the curves was not totally maintained: The portion of the vesicular domain corresponding to stage Ia gradually decreased with decreasing HSPC concentration and, consequently, it was not possible to fully assess the behaviour in the vesicular stage. The boundary phase parameters were calculated from the characteristic points (Table 1) and the phase diagram obtained (Fig. 6). Due to its negative deviation, the absorbance corresponding to a lipid concentration of 0.4 mM was rejected. This change in the expected value has been described by other authors<sup>34,35</sup> at very low lipid concentration using pure bile salts, and taking into account the finite size of mixed micelles and the end-cap effect of cylindrical micelles. Size analysis (Fig. 3) also reflects the complete solubilisation of HSPC liposomes at  $55^\circ\text{C}$ : A mean diameter close to 10 nm was observed at the end of the process, indicating the mere existence of mixed micelles.

265

3.3 HSPC/CHOL liposomes

DSC thermograms of HSPC/CHOL liposomes showed the abolition of the phase transition temperature (data not shown) measured in pure HSPC samples. This fact indicates that a homogeneous liquid-ordered membrane was obtained. Figure 7 corresponds to the incubation of HSPC/CHOL liposomes with BSE. It can be observed that there was a sharp initial decrease of the absorbance at low BSE concentrations, and a subsequent constant value (0.22) at half the initial absorbance. There was a concomitant decrease in the fluorescence (Fig. 7), and the minimum value (32% of the initial value) was reached at a BSE concentration of about 2 mM. Consequently, and similarly to SPC and HSPC, the interaction of bile salts with HSPC/CHOL liposomes at low BSE to lipid ratios increased the bilayer permeability of the vesicles. Both the constant value of the absorbance and the diameter evolution (Fig. 3) obtained at higher BSE concentrations reveal that liposomes were not solubilised, as described for HSPC vesicles. Surprisingly, and contrary to the incubations performed with SPC and HSPC liposomes, a residual fluorescence was maintained once the absorbance reached a plateau (about 50% of the initial fluorescence). This remarkable resistance of HSPC/CHOL liposomes to solubilisation is evident in Figure 8: Not even diluted liposomes (0.25 mM total lipid) at the highest BSE concentration (56 mM) were solubilised during the incubation, only decreasing the absorbance to 50% of the initial value. The curves corresponding to phospholipid concentrations of 0.76 and 1 mM (Fig. 8) clearly show the stage at which pyranine was initially released. In this zone, there was an initial decrease of the absorbance upon increasing the BSE concentration which was concomitant with a vesicle size diminution (Fig. 3), and the subsequent absorbance increase was also associated with a diameter increase. This behaviour parallels that observed with SPC liposomes, and could be indicative of similar mechanisms of

interaction of BSE with the two types of bilayers, that is, the existence of Ia and Ib stages.

In order to achieve full solubilisation of HSPC/CHOL liposomes in 1-2 hours the temperature had to be raised to 65°C. The results (Figure 9) show the complex  
295 behaviour of the system, with some consecutive absorbance peaks before the onset of solubilisation. Consequently, unlike that which occurs with SPC and HSPC, more than two vesicular sub-domains can be considered for HSPC/CHOL liposomes when they interact with BSE if all the break points of the absorbance plots are taken into account. Unfortunately, the profiles of the curves were similar only for the higher lipid  
300 concentrations used, thus it was not possible to obtain the equivalent characteristic points for all the lipid concentrations.

This fact conditioned the calculation of the boundary phases and explains the existence of a negative value of  $[\text{BSE}]_w^{\text{sat}}$  (Table 1) which is, obviously, a consequence of the experimental error of the extrapolation. For this reason Table 1 shows the data  
305 corresponding to the stages II and III which are complemented in the inset of Fig. 9 with some other points of the vesicular domain. Note that, as for the cases of SPC and HSPC, some characteristics points corresponding to vesicular stages at low phospholipid concentrations showed deviations from linearity and were excluded in the linear regression fit. As regards the vesicle size analysis, the mean diameter determined after  
310 full solubilisation was about 200 nm (% volume average). However, the measured mean diameter expressed as % number average was 20 nm. These results provide evidence of the heterogeneity of the sample at this stage, although both the absorbance value and the diameter obtained from the number distribution indicate that a large quantity of the initial liposomes was solubilised.

315

#### 4 DISCUSSION

The experimental design used in the present work combines, on the one hand, absorbance and size measurements that can explain the changes that take place during the interaction of BSE with liposomes. On the other hand, the fluorescence experiments provide information on how the membrane permeability/integrity is affected during this process. As it is known, the *in vivo* effectiveness of the liposomes depends on the interaction with bile salts, on lipid digestion, and also on the solubilisation of the incorporated drug, and possible enhancement of permeability. Consequently, our study provides specific information which could partially explain the *in vivo* effectiveness of liposomes as oral drug delivery systems.

From the results obtained by the incubation of SPC vesicles with a natural BSE for 1 h at 37°C, three primary conclusions may be reached: a) SPC liposomes can be efficiently solubilised in these conditions; b) their aqueous content can be completely released to the bulk, even if no destruction of the molecular structure of the vesicle has taken place and; c) at very low BSE to lipid ratios (stage Ia) the aqueous content is maintained, although an interaction between BSE and liposomes is detected.

The observed effect of BSE on phosphatidylcholine liposomes (Fig. 1, 2, and 3) gave similar absorbance results to that obtained by Andrieux et al.<sup>23</sup> and Elsayed and Cevc<sup>21</sup> using pure bile salts. These authors performed a continuous slow addition of taurocholate (TC) or worked in equilibrium conditions using cholate (C), respectively.

In our case, before the onset of solubilisation (that is, in the vesicular domain) BSE first causes a strong decrease of the absorbance and then a small increase. This behaviour parallels the previously mentioned works and, therefore, a similar explanation of the vesicular changes could be proposed. Elsayed and Cevc<sup>21</sup> explained these absorbance results by both a vesicle-apparent shrinkage caused by bilayer fluctuations induced by



the surfactant (which would produce a decrease in the absorbance), and an expansion of the membrane and an increase of the vesicle size caused, merely, by its insertion into the membrane (which would cause an increase in the absorbance). Consequently, as they said, there is a counter-play between both phenomena, which would explain the negative and positive slopes of the absorbances observed at stages Ia and Ib, respectively.

If we now consider our fluorescence results, it can be demonstrated that SPC bilayers remain stable while they interact with the BSE during stage Ia (more than 80% of the fluorescence is retained). As the molar fraction  $x^{BSE,Ia}_{agg}$  is 0 mM, it can be concluded that in the stage Ia there is no insertion of BSE into the bilayers. This scenario is compatible with the hypothesis of Andrieux et al.<sup>23</sup> who proposed that, in the first range of the vesicular domain, TC monomers are located at the phospholipid-water interface with no interaction with the hydrophobic core of the membrane. The results observed in our work suggest that this arrangement can be also applied to all the BSE components in the Ia stage: The non-existence of surfactant insertion during the incubation ensures the retention of the probe by preserving the permeability of the liposomal membrane.

However, it is obvious that the changes in absorbance and mean diameter measured in the entire vesicular domain provide evidence that there are variations of the liposome shape and/or size. Such variations only affect membrane permeability during stage Ib (pyranine is released), that is, when the bilayer expansion caused by the insertion of the bile salts causes the positive slope of the absorbance. In a recent work, Niu et al.<sup>36</sup> evaluated the effectiveness of insulin-loaded liposomes that contained several bile salts using a phospholipid (SPC) to bile salt molar ratio of 4:1. The increased transport of insulin observed by the authors in Caco-2 cell cultures is compatible with the existence

365 of liposomes in the Ib stage, that is, the vesicular structure is maintained, and at the same time they gradually release their content into the medium.

As can be seen in Table 1, BSE exhibits an increased effectiveness of solubilisation compared with some pure bile salts. The  $[\text{detergent}]_w^{\text{sat}}$  values obtained by other authors using phosphatidylcholine (PC) liposomes in saline medium are 1.4 mM for 370 deoxycholate (DC) and 6 mM for C (large unilamellar liposomes, 30°C),<sup>37</sup> and 3 mM for TC (small unilamellar liposomes, 25°C).<sup>23</sup> In our experiments, a smaller value was obtained ( $1.24 \pm 0.14$  mM), and as  $[\text{detergent}]_w^{\text{sat}}$  increases with temperature,<sup>37</sup> it can be shown that at 37°C BSE mixed micelles are formed at a lower concentration than the mentioned pure bile salts. The  $R_e^{\text{sat}}$  value obtained with BSE ( $0.39 \pm 0.07$ ) is similar to 375 that achieved with DC (0.35), C (0.33) and TC (0.29) by the same previous authors.<sup>23,37</sup> Thus, at a given lipid concentration, the maximum quantity of BSE, DC, C and TC in the liposome membranes before the formation of mixed micelles is approximately the same. As expected, and instead of being equal,  $[\text{BSE}]_w^{\text{sol}} > [\text{BSE}]_w^{\text{sat}}$  as usually occurs with bile salts due to intermicellar interactions and its value ( $4.58 \pm 0.12$  mM) is located 380 between that of TC (4 mM)<sup>23</sup>, C (from 5 to 8 mM)<sup>21,37</sup> and DC (2 mM)<sup>37</sup>. With reference to  $R_e^{\text{sol}}$ , the value obtained for BSE ( $1.60 \pm 0.06$ ) is higher than that obtained with the previous bile salts. This fact means that the minimum molar fraction of BSE necessary to transfer all the PC into mixed micelles (0.62) about 30% higher than that of C (0.47),<sup>21</sup> which, in turn, is higher than DC and TC.

385 The observed effect of BSE on PC liposomes is not conclusive when compared to *in vitro* digestions carried out with simulated complex intestinal fluids instead of pure bile salts. Literature shows contradictory results<sup>14,38</sup> which could be caused by the different grade of purity of the PC used, as well as the different lipid digestion models.

Taking into account the previous facts, it can be concluded that PC liposomes,  
390 characterised by their fluid state membrane, are greatly susceptible to release all their  
entrapped aqueous content during intestinal digestion due to the effect of bile salts. The  
very small range of stage Ia hardly ensures the maintenance of the water soluble  
entrapped molecules. By contrast, stage Ib and (obviously) partial and full liposome  
solubilisation, lead to the total release of the aqueous core to the medium. This  
395 behaviour can be an advantage if lipophilic substances are incorporated into the  
liposome bilayer. In these cases, if the membrane fluidity is not altered, vesicles will be  
solubilised into mixed micelles which would increase the intestinal uptake.

The behaviour of HSPC liposomes upon incubation is totally different from that of SPC  
vesicles. The results shown in Figures 3, 4 and 5 indicates that stage Ib is the main one  
400 in the vesicular domain and that full solubilisation of liposomes is not achieved under  
the reported conditions. Consequently, large mixed structures are formed instead of  
micelles, even at high BSE to HSPC ratios. The fluorescence and absorbance results are  
compatible with those observed by Andrieux et al.<sup>20</sup> in DSC experiments performed  
with dipalmitoylphosphatidylcholine (DPPC) liposomes under the continuous addition  
405 of TC. They detected a decrease in the fusion enthalpy of membranes as a consequence  
of TC insertion in the vesicular domain, and concluded that in those conditions (before  
the phase transition temperature) the DPPC gel-phase exhibits a disordered state when  
TC is present into the bilayer. In our case, this proposed pre-transition disordered state,  
caused by a rapid insertion of bile salts into the membranes, is consistent with both the  
410 dramatic morphological changes evidenced by the absorbance changes and the intense  
pyranine leakage. On the contrary, when the concentration of TC is increased, Andrieux  
et al.<sup>20</sup> achieve a full liposome solubilisation at 37°C, that is, below the phase transition  
temperature of DPPC ( $T_m=41^\circ\text{C}$ ), a phenomenon that is not observed in our HSPC

liposomes. This different behaviour could be caused by the transition temperature of  
415 HSPC ( $T_m=51.8\pm 0.2^\circ\text{C}$ ,  $n=4$ ). This hypothesis is compatible with the results obtained by  
Kokkona et al.<sup>39</sup> They performed incubation experiments (1 h,  $37^\circ\text{C}$ ) with 10 mM C or  
TC and 2.5 mM DPPC or distearoylphosphatidylcholine (DSPC,  $T_m=55^\circ\text{C}$ ) liposomes  
and found that around 15% and 20% of the entrapped dye remained in DPPC and DSPC  
vesicles, respectively. Therefore, C and TC highly modified bilayer permeability but did  
420 not solubilise the liposomes. In our case, the effect of BSE on bilayer permeability is  
higher than that caused by TC and C alone, due to the fact that the dye is completely  
released to the bulk. But the high transition temperature of HSPC liposomes, similar to  
that of DSPC, could explain their resistance to solubilisation.

Solubilisation of HSPC liposomes by bile salts was found to be dependent on the  
425 temperature. Full vesicle solubilisation can be achieved at  $55^\circ\text{C}$  (Fig. 3 and 6), that is,  
when the membrane is in the fluid state. In this conditions  $[\text{BSE}]_w^{\text{sat}}$  ( $3.55\pm 0.74$  mM)  
and  $[\text{BSE}]_w^{\text{sol}}$  ( $7.37\pm 0.43$  mM) are similar to that obtained by Hildebrand et al.<sup>34</sup> with  
DPPC liposomes, in saline, with C and at  $60^\circ\text{C}$  (5.6 mM and 6.6 mM respectively). On  
the other hand, the slopes of BSE (Table 1) are one order of magnitude higher than that  
430 of C. This fact could be a consequence of the transition temperature of the phospholipid:  
It is known that solubilisation of dimyristoylphosphatidylcholine ( $T_m=24^\circ\text{C}$ ) liposomes  
with C at  $30^\circ\text{C}$  shows slopes 10 times smaller than that of DPPC.<sup>34</sup>

In light of what has been previously said, HSPC liposomes used in oral formulations  
would release all the entrapped water-soluble substances during their interaction with  
435 bile salts. In presence of BSE, and although they cannot be solubilised by it, the  
organisation of the gel-state bilayers is drastically altered, resulting in an increased  
permeability and, finally, mixed nano/microstructures. For this reason, if lipophilic

substances were included in the bilayers, they would not be as efficiently transferred to mixed micelles, as in the case of SPC liposomes.

440 From the results obtained with HSPC/CHOL liposomes (Fig. 3, 7 and 8) it can be inferred that the incubations performed at 37°C and with high BSE concentrations resulted in mixed vesicles, which keep part of their initial entrapped aqueous volume: Despite the significant morphological changes, they retained a high percentage of the entrapped fluorescent dye. This behaviour markedly contrasts with that of fluid (SPC) 445 and gel-state (HSPC) liposomes at 37°C and provides evidence that the liquid-ordered bilayer of HSPC/CHOL vesicles can undergo a very particular interaction with the BSE bile salts during the intestinal digestion.

In this regard, the morphological changes of HSPC/CHOL liposomes that cause a decrease in the absorbance (Fig. 8) and mean diameter (Fig. 3) (characteristic events of 450 the Ia stage) are correlated with a leakage of the entrapped dye (Fig. 7). Note that this was not the behaviour of SPC liposomes during the Ia stage, where practically no release of HTPS nor insertion of the surfactants into the bilayers were detected. This fact suggests that, during the vesicle-apparent shrinkage of the HSPC/CHOL liposomes, a surfactant insertion into the liquid-ordered bilayers takes place. At higher BSE 455 concentrations, when a subsequent increase of the vesicle size is produced (stage Ib), the loss of the fluorescent dye ends, just the opposite of that which occurs with SPC and HSPC liposomes. Therefore, there is a critical inserted-surfactant to lipid ratio that leads to a strong stabilisation of the HSPC/CHOL membrane (Fig.8) and prevents the loss of the entrapped aqueous medium. Accordingly, HSPC/CHOL liposomes were definitely 460 the most resistant vesicles to a complex natural mixture of bile salts, as demonstrated by the fact that they were only solubilised at high bile extract to lipid ratios and elevated temperatures (Table 1 and Fig. 3 and 9). As can be observed in the Inset of Fig. 9, at

low lipid concentrations there were large deviations from linearity, and this fact prevented the precise determination of the vesicular sub-domains.

465 Consequently, if HSPC/CHOL liposomes are used in oral applications, it is expected that during the intestinal digestion they would maintain part of their entrapped aqueous material and would preserve, partially, their vesicular structure. This particular behaviour has to be due to their liquid-ordered molecular organisation, induced by cholesterol, and, therefore, could be also caused by other lipophilic molecules that, at  
470 the same time, could be of pharmacological interest. This could be the case, for example, of phytosterols, which have a very similar structure to cholesterol. In this sense, it has been shown that, in mixtures with DPPC, some of those vegetable sterols cause a similar phase behaviour to that caused by cholesterol, and also induced, in different degrees, an increase of the bilayer thickness.<sup>40</sup>

475

## 5 CONCLUSIONS

The present work shows that each one of the three liposome preparations assayed show different types of interaction with natural BSE at the human physiological concentration  
480 range, that is, from 4 mM to 11 mM, pH 6.5 and 37°C. As all the vesicles contained a phospholipid with a common headgroup (choline) the different behaviour can be attributed mainly to the difference in their membrane status (fluid, gel-state and liquid-ordered bilayers). These particular responses to physiological bile salts should be taken into account when designing liposome formulations as drug carriers. They also indicate  
485 that each type of vesicle offers singular features that can be useful in oral delivery systems. Thus, our findings may be useful for investigators developing liposomal delivery systems in oral form, which is our main objective.

490 **Acknowledgements**

This research was supported (PTR95-0480-OP) by the Ministry of Science and Technology of Spain. The authors would like to thank Dr. Josep Cladera for helpful comments and suggestions.

## REFERENCES

- 495 1. R. R. Sawant and V. P. Torchilin, *Soft Matter*, 2010, 6, 4026–4044.
2. M. Malmsten, *Soft Matter*, 2006, 2, 760–769.
3. G. Fricker, T. Kromp, A. Wendel, A. Blume, J. Zirkel, H. Rebmann, C. Setzer, R.O. Quinkert, F. Martin, and K. Müller-Goymann, *Pharm. Res.*, 2010, 27, 1469–1486.
4. P. Guan, Y. Lu, J. Qi, M. Niu, R. Lian, F. Hu and W. Wu, *Int.J. Nanomed.*, 2011, 6,  
500 965–974.
5. S.K. Bobbala and, P.R. Veerareddy, *J. Liposome Res.*, 2012, 22, 285–294.
6. P. N. Gupta and S.P.Vyas, *Colloid. Surface B*, 2011, 82, 118–125.
7. W. Liu, A. Ye, W. Liu, C. Liu and H. Singh, H., *J. Dairy Sci.*, 2013, 96, 2061–2070.
8. Y. Dai, R. Zhou, L. Liu, Y. Lu, J. Qi and W. Wu, *Int.J. Nanomed.*, 2013, 8, 1921–  
505 1933.
9. A. Macierzanka, N. M. Rigby, A. P. Corfield, N. Wellner, F. Böttger, E. N.C. Millsa and A.R. Mackie, *Soft Matter*, 2011, 7, 8077–8084.
10. J.S. Dempe, R.K. Scheerle, E. Pfeiffer and M. Metzler, *Mol. Nutr. Food Res.*, 2013, 57, 1543–1549.
- 510 11. L.G. Hermida, A. Roig, C. Bregni, M. Sabés-Xamaní and R. Barnadas-Rodríguez, *J. Liposome Res.*, 2011, 21, 203–212.
12. A. Patel, Y. Hu, J.K. Tiwari and K.P. Velikov, *Soft Matter*, 2010, 6, 6192–6199.
13. R.P. Glahn, C. Lai, J. Hsu, J.F. Thompson, M. Guo and D.R. van Campen, *J. Nutr.*, 1998, 128, 257–264.
- 515 14. L.G. Hermida, M. Sabés-Xamaní and R. Barnadas-Rodríguez, *J. Liposome Res.*, J. Liposome Res., 2009, 19, 207–219.



15. M. Jovaní, R. Barberá, R. Farré and E. Martín-de-Aguilera, *J. Agric. Food Chem.*, 2001, 49, 3480–3485.
16. R.P. Glahn, O.A. Lee, A. Yeung, M.I. Goldman and D.D. Miller, *J. Nutr.*, 1998,  
520 128, 1555–1561.
17. V.N. Ngassam, M.C. Howland, A. Sapuri-Butti, N. Rosidic and A.N. Parikh, *Soft Matter*, 2012, 8, 3734–3738.
18. U. Kragh-Hansen, M. le Maire and J.V. Moller, *Biophys. J.*, 1998, 75, 2932–46.
19. D. Levy, A. Gulik, M. Seigneuret and J.L. Rigaud, *Biochemistry*, 1990, 29, 9480–  
525 9488.
20. K. Andrieux, L. Forte, S. Lesieur, M. Paternostre, M. Ollivon and C. Grabielle-Madelmont, *Eur. J. Pharm. Biopharm.*, 2009, 71, 346–55.
21. M.M. Elsayed and G. Cevc, *Biochim. Biophys. Acta*, 2011, 1808, 140–53.
22. E. Schnitzer, M.M. Kozlov and D. Lichtenberg, *Chem. Phys. Lipids*, 2005, 135, 69–  
530 82.
23. K. Andrieux, L. Forte, S. Lesieur, M. Paternostre, M. Ollivon and C. Grabielle-Madelmont, *Pharm. Res.*, 2004, 21, 1505–16.
24. A. Hildebrand, K. Beyer, R. Neubert, P. Garidel, and A. Blume, *J. Colloid Interf. Sci.*, 2004, 279, 559–571.
- 535 25. D. Wustner, A. Herrmann and P. Muller, *J. Lipid Res.*, 2000, 41, 395–404.
26. M. R. Vist and J. H. Davis, *Biochemistry*, 1990, 29, 451–464.
27. *The structure of biological membranes*, Philip Yeagle Ed., CRC Press, 1992.
28. U. Gustafsson, S. Sahlin and C. Einarsson, *World J. Gastroentero.*, 2003, 9, 1576–1579.

- 540 29. M.D. Yago, V. González, P. Serrano, R. Calpena, M.A. Martínez, E. Martínez-Victoria and M. Mañas, M., *Nutrition*, 2005, 21, 339–347.
30. R. Barnadas-Rodríguez and M. Sabés-Xamaní, *Method. Enzymol.*, 2003, 367, 28–46.
31. D. Lichtenberg, R.J. Robson and E.A.. Dennis, *Biochim. Biophys. Acta*, 1983, 737,  
545 285–304.
32. M. Paternostre, O. Meyer, C. Grabielle-Madelmont, S. Lesieur, M. Ghanam and M. Ollivon, *Biophys. J.*, 1995, 69, 2476–88.
33. M. Ueno, *Biochemistry*, 1989, 28, 5631-5634.
34. A. Hildebrand, R. Neubert, P. Garidel and A. Blume, *Langmuir*, 2002, 18, 2836–  
550 2847.
35. Y. Roth, E. Opatowski, D. Lichtenberg and M.M. Kozlov, *Langmuir*, 2000, 16, 2052–2061.
36. M. Niu, Y. Tan, P. Guan, L. Hovgaard, Y. Lu, J. Qi, R. Lian, X. Li and W. Wua, *Int. J. Pharm.*, 2014, 460, 119–130.
- 555 37. A. Hildebrand, K. Beyer, R. Neubert, P. Garidel and A. Blume, *Colloid. Surface B*, 2003, 32, 335–351.
38. W. Liu, A. Ye, C. Liu, W. Liu and H. Singh, *Food Res. Int.*, 2012, 48, 499–506.
39. M. Kokkona, P. Kallinteri, D. Fatouros and S.G. Antimisiaris, *Eur. J. Pharm. Sci.*, 2000, 9, 245-252.
- 560 40. Md. Arif Kamal and V. A. Raghunathan, *Soft Matter*, 2012, 8, 8952–8958.

**FIGURE CAPTIONS**

565 **Figure 1.** Absorbance (circles) and fluorescence (squares) changes of suspensions of SPC liposomes (0.60 mM) in the presence of BSE after 1 h of incubation at 37°C. The inset corresponds to low concentrations of BSE.

**Figure 2.** Solubilisation curves of SPC liposomes (circle: 3.33 mM; square: 2.33 mM; up triangle: 1.75 mM; down triangle: 0.88 mM; diamond: 0.60 mM) obtained in the presence of BSE after 20 min at 37°C. Inset: Phase diagram of SPC/BSE mixtures obtained from the solubilisation curves. (\*: Point rejected).

**Figure 3.** Effect of BSE concentration on the mean diameter (%volume distribution) after 1 hour of incubation of SPC (circle: 1.8 mM, 37°C), HSPC (dark square: 1.2 mM, 37°C; white square: 3.3 mM, 55°C), and HSPC/CHOL liposomes (dark up triangle: 1.1 mM, 37°C; white up triangle: 1 mM, 65°C). Mean diameter of HSPC/CHOL liposomes incubated with 56 mM BSE at 65°C is also expressed as number distribution (white down triangle).

580

**Figure 4.** Absorbance (circle) and fluorescence (square) changes of suspensions of HSPC liposomes (0.67 mM) in the presence of BSE after 1 h of incubation at 37°C.

**Figure 5.** Effect of BSE concentration after 1 hour incubation at 37°C on the absorbance of HSPC liposomes (circle: 3.33 mM; red square: 2.13 mM; up triangle: 1.24 mM; down triangle: 0.67 mM; diamond: 0.40 mM).

585

**Figure 6.** Solubilisation curves of HSPC liposomes (circle: 3.33 mM; square: 2.13 mM; up triangle: 1.24 mM; down triangle: 0.67 mM; diamond: 0.40 mM) obtained in the presence of BSE after 1 h at 55°C. Inset: Phase diagram of HSPC/BSE mixtures obtained from the solubilisation curves. (\*: Point rejected).

**Figure 7.** Absorbance (circle) and fluorescence (square) changes of suspensions of HSPC/CHOL liposomes (0.5 mM) in the presence of BSE after 1 h incubation at 37°C.

595

**Figure 8.** Effect of BSE concentration on the absorbance of HSPC/CHOL liposomes (black circle: 1.04 mM; square: 0.76 mM; up triangle: 0.5 mM; down triangle: 0.36 mM; diamond: 0.25 mM) after 1 hour incubation at 37°C.

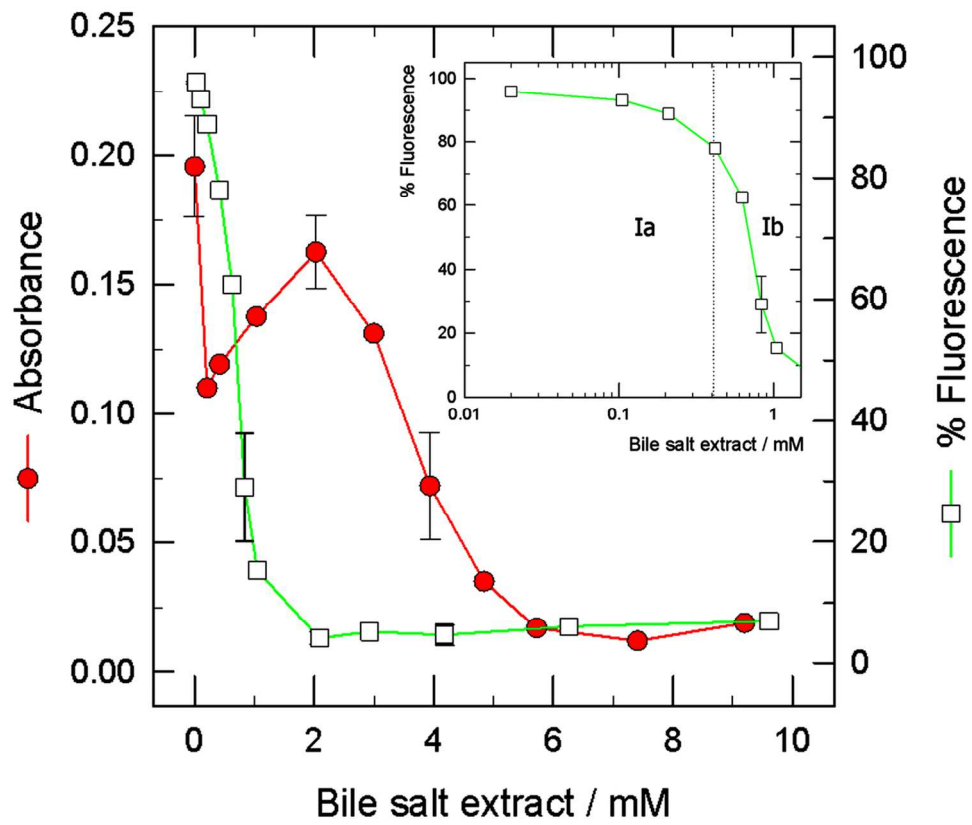
**Figure 9.** Solubilisation curves of HSPC/CHOL liposomes (circle: 1.04 mM; square: 0.76 mM; up triangle: 0.5 mM; down triangle: 0.36 mM; diamond: 0.25 mM) obtained in the presence of BSE after 1 h at 65°C. Inset: Phase diagram of HSPC/CHOL/BSE mixtures obtained from the solubilisation curves. (\*: Points rejected).

600

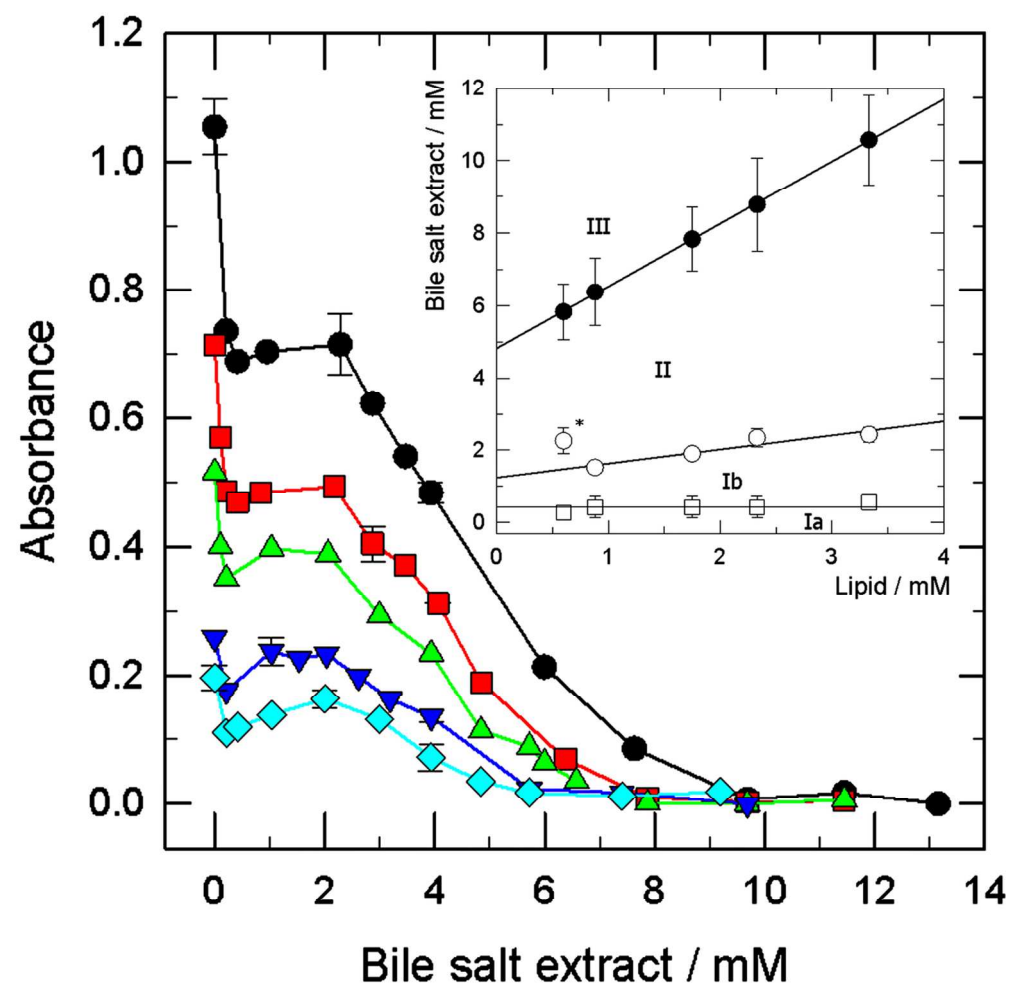
**Table 1.** Solubilisation parameters of SPC, HSPC and HSPC/CHOL liposomes obtained by incubation with BSE.

| Composition | Temperature (°C) | Inc. time | $C_{lab}$            |             |                     | $C_{sat}$            |             |                 | $C_{sol}$            |             |                     |
|-------------|------------------|-----------|----------------------|-------------|---------------------|----------------------|-------------|-----------------|----------------------|-------------|---------------------|
|             |                  |           | $[BSE]_w^{lab}$ (mM) | $R_e^{lab}$ | $x^{BSE,lab}_{agg}$ | $[BSE]_w^{sat}$ (mM) | $R_e^{sat}$ | $x^{BSE}_{agg}$ | $[BSE]_w^{sol}$ (mM) | $R_e^{sol}$ | $x^{BSE,sol}_{agg}$ |
| SPC         | 37               | 20 min    | 0.41±0.23            | 0           | 0                   | 1.24±0.14            | 0.39±0.07   | 0.28            | 4.58±0.12            | 1.60±0.06   | 0.62                |
| HSPC        | 55               | 1 h       | 3.1±1.3              | 0           | 0                   | 3.55±0.74            | 1.58±0.35   | 0.61            | 7.37±0.43            | 5.07±0.8    | 0.84                |
| HSPC/CHOL   | 65               | 1-2 h     | -                    | -           | -                   | -1.1± 2.3            | 22.9±3.6    | 0.96            | 1.24±1.46            | 43.0±2.6    | 0.98                |

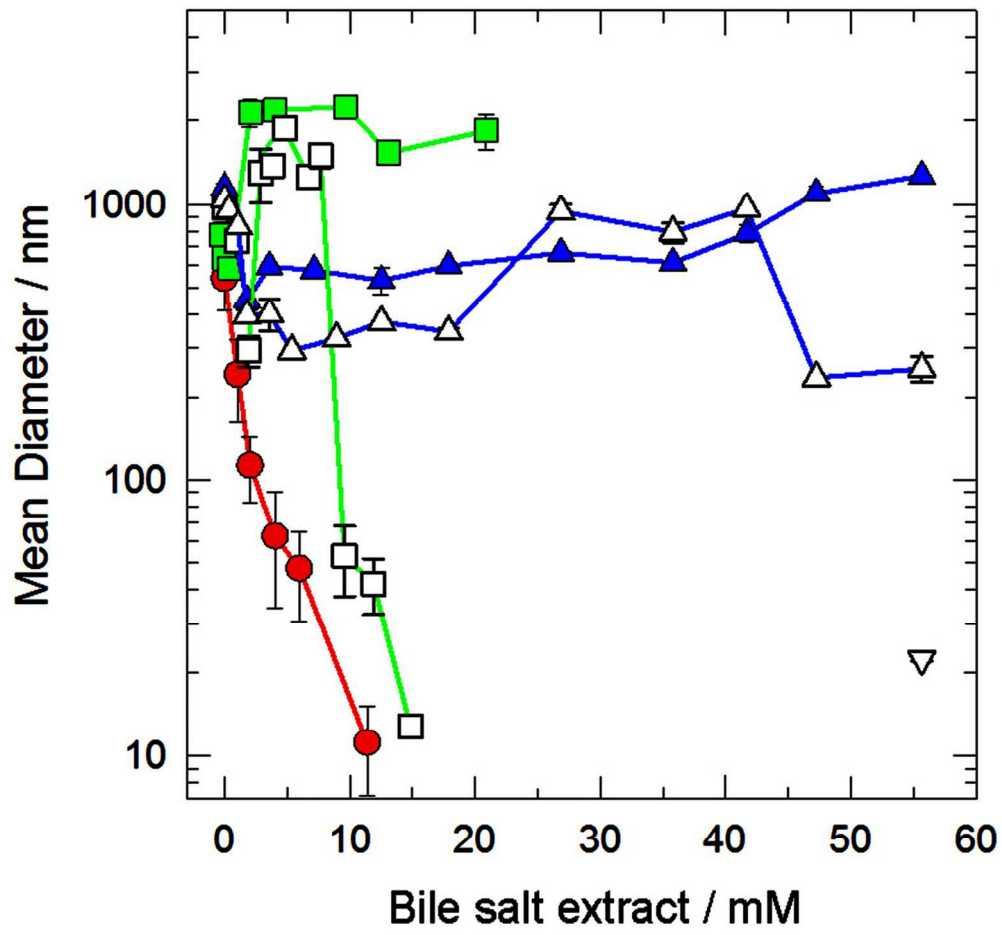
605



123x104mm (300 x 300 DPI)

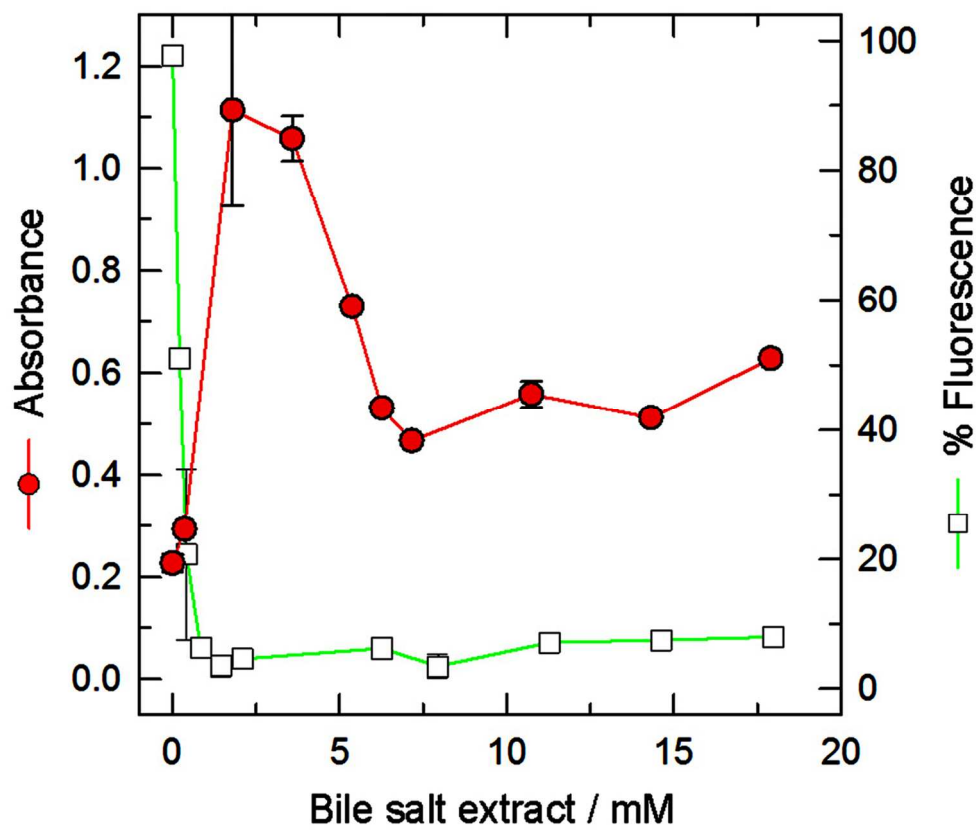


123x125mm (300 x 300 DPI)

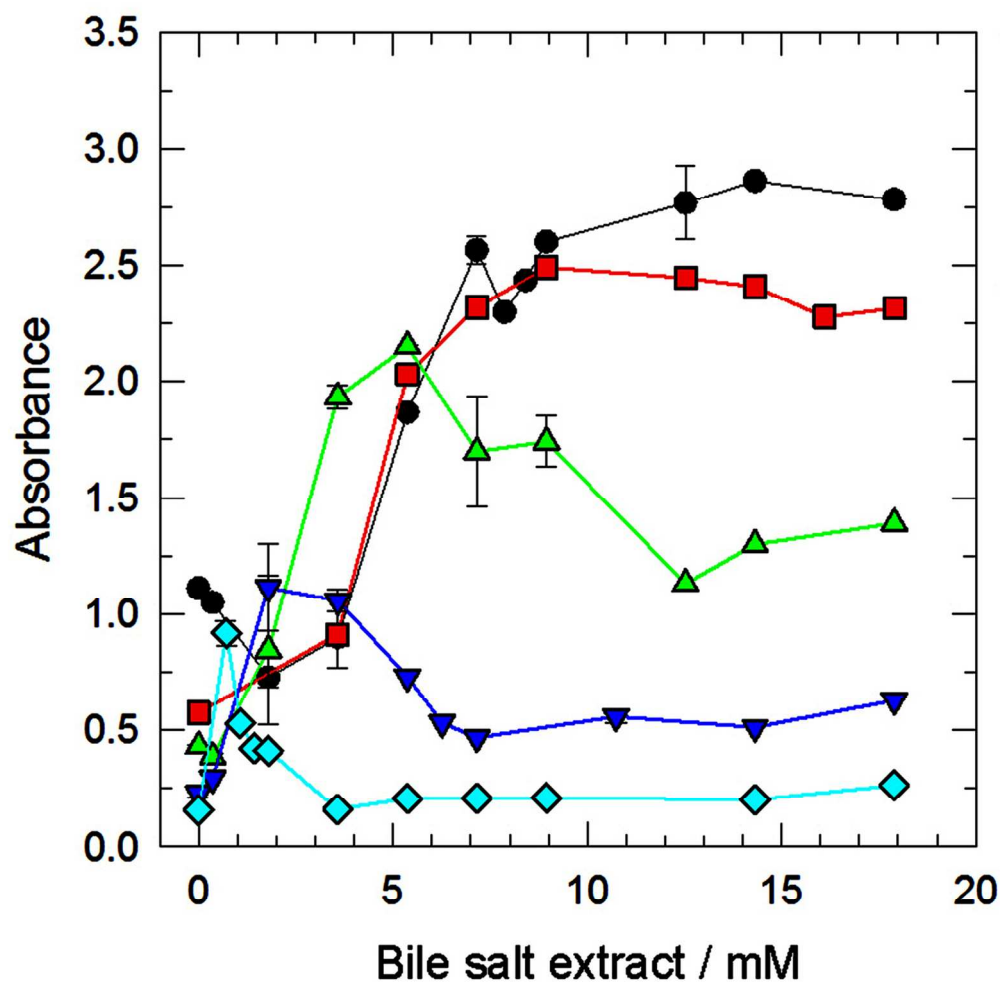


122x117mm (300 x 300 DPI)

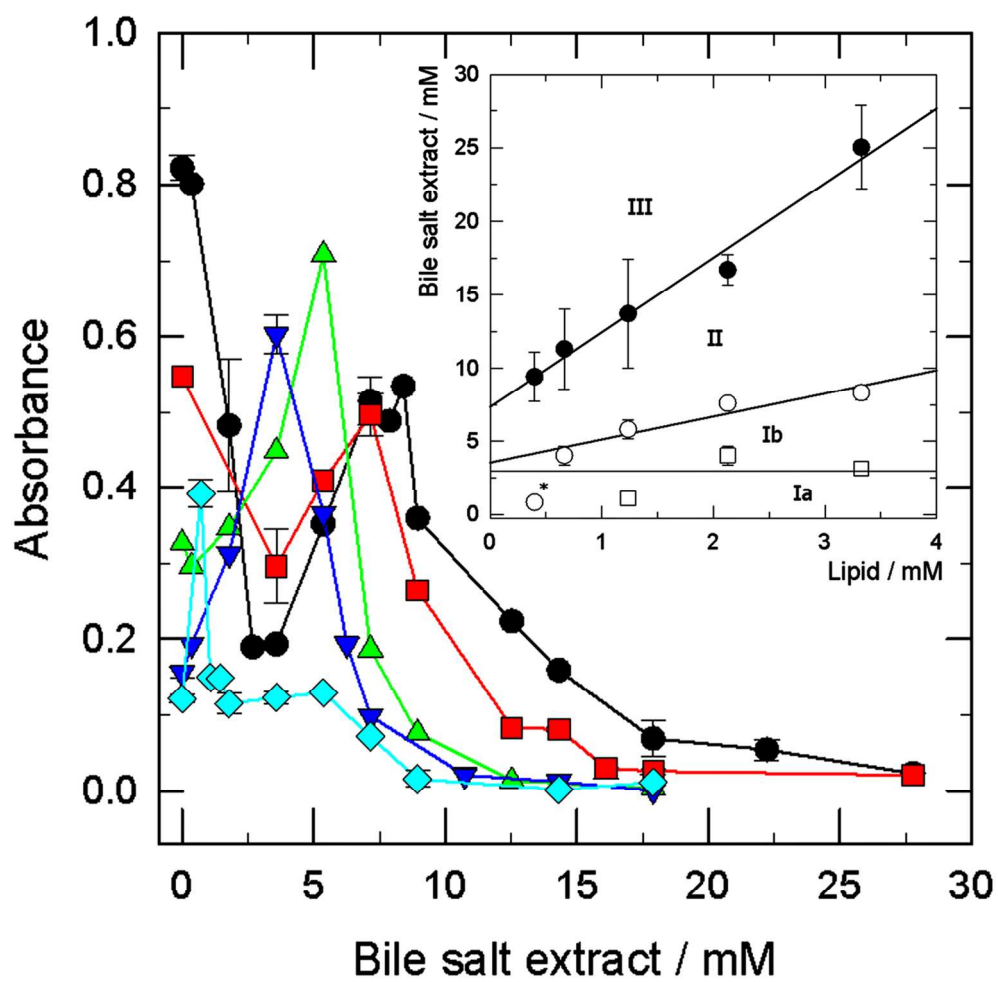




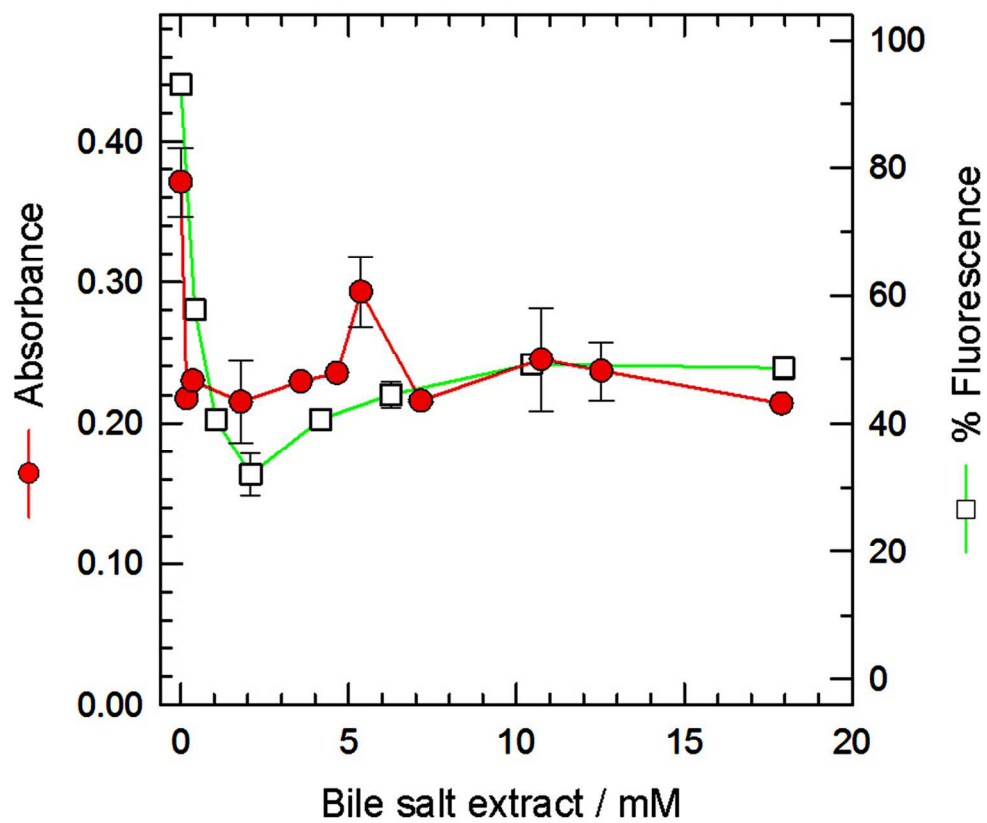
120x101mm (300 x 300 DPI)



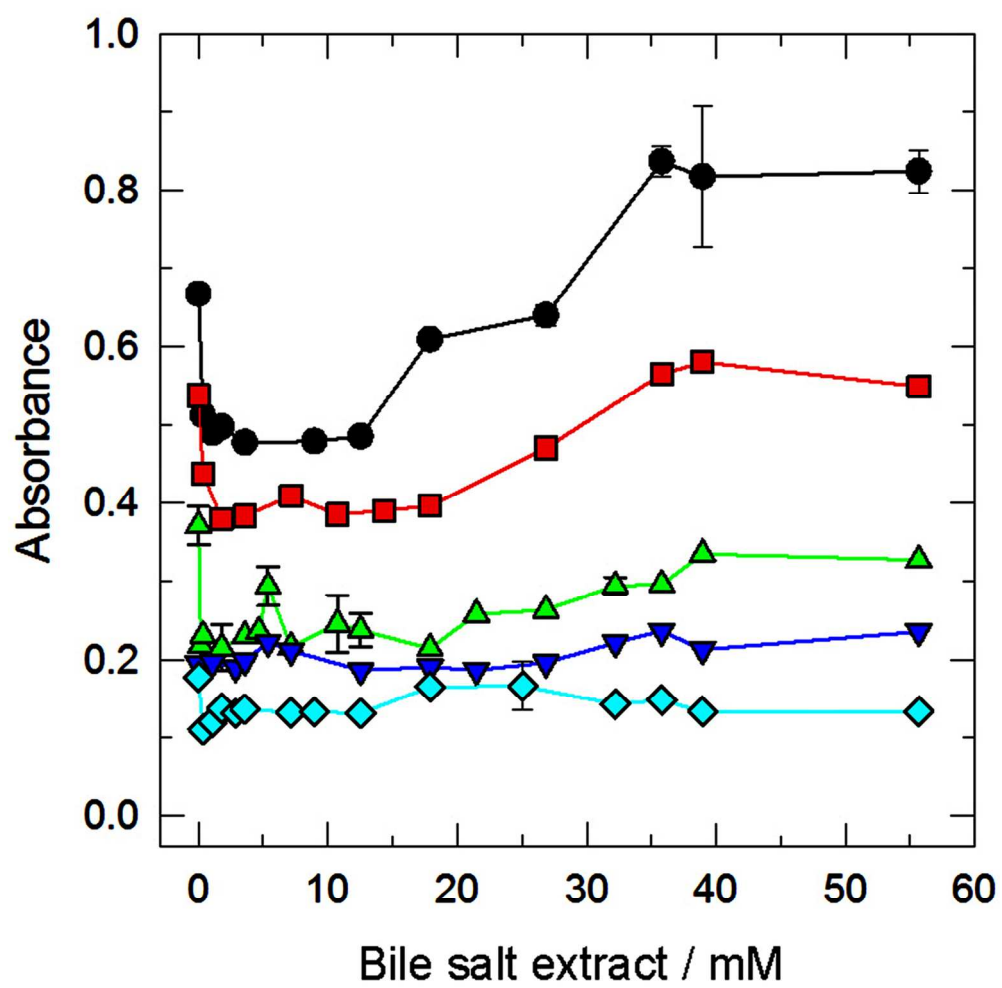
122x122mm (300 x 300 DPI)



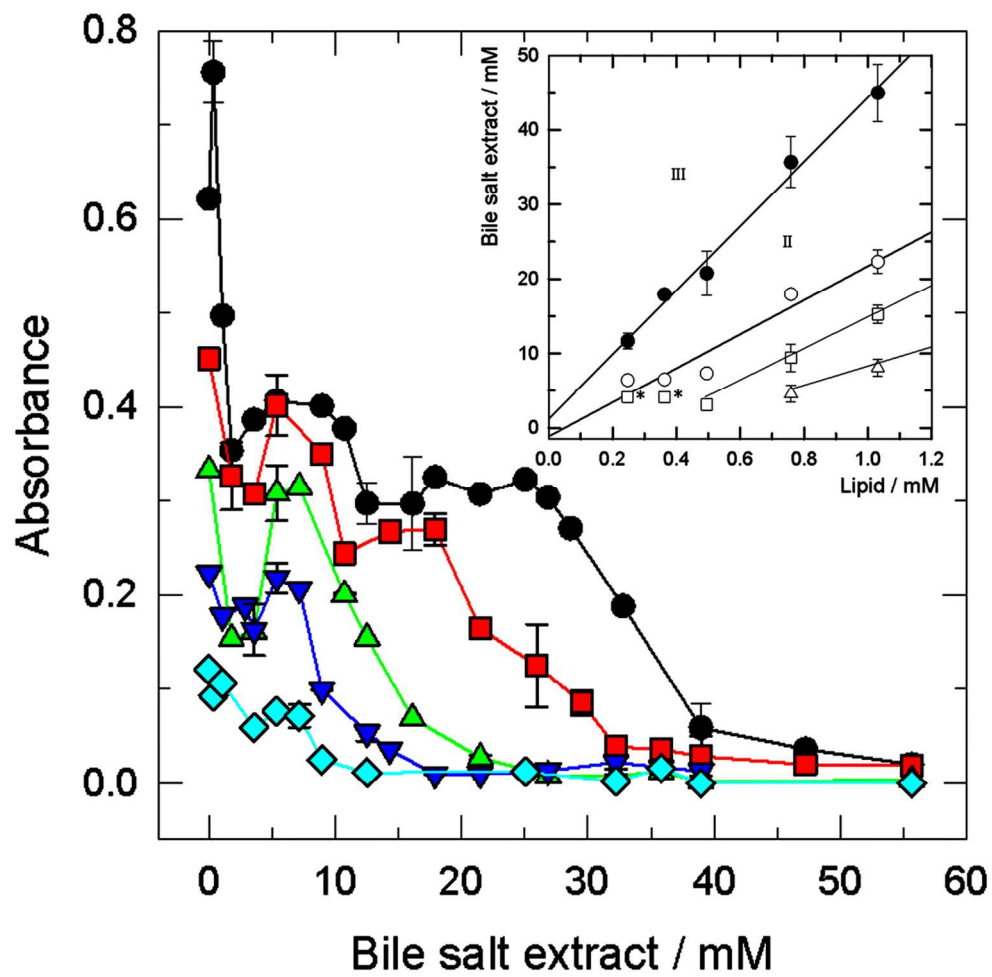
122x122mm (300 x 300 DPI)



124x107mm (300 x 300 DPI)



123x123mm (300 x 300 DPI)



120x117mm (300 x 300 DPI)